The core anammox redox reaction system of 12 anammox bacterial genera and their evolution and application implications

Hu, Pengfei; van Loosdrecht, Mark; Gu, Ji Dong; Yang, Yuchun

DOI
10.1016/j.watres.2025.123551

Publication date
2025

Document Version
Final published version

Published in
Water Research

Citation (APA)
Hu, P., van Loosdrecht, M., Gu, J. D., & Yang, Y. (2025). The core anammox redox reaction system of 12 anammox bacterial genera and their evolution and application implications. *Water Research*, *281*, Article 123551. https://doi.org/10.1016/j.watres.2025.123551

Water Research 281 (2025) 123551

Contents lists available at ScienceDirect

Water Research

journal homepage: www.elsevier.com/locate/watres

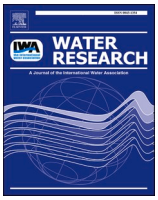

The core anammox redox reaction system of 12 anammox bacterial genera and their evolution and application implications

Pengfei Hu [a,b], Mark van Loosdrecht [c], Ji-Dong Gu [a,b,d,*], Yuchun Yang [e,*]

[a] Environmental Science and Engineering Research Group, Guangdong Technion-Israel Institute of Technology, 241 Daxue Road, Shantou, Guangdong 515063, PR China
[b] Civil and Environmental Engineering, Technion – Israel Institute of Technology, Haifa 320003, Israel
[c] Department of Biotechnology, Delft University of Technology, Van der Maasweg 9 2629 HZ Delft, the Netherlands
[d] Guangdong Provincial Key Laboratory of Materials and Technologies for Energy Conversion, Guangdong Technion - Israel Institute of Technology, 241 Daxue Road, Shantou, Guangdong 515063, PR China
[e] State Key Laboratory of Biocontrol, School of Ecology, Shenzhen Campus of Sun Yat-sen University, Shenzhen, Guangdong, 518107, PR China

ARTICLE INFO

Keywords:
Anammox reaction
Electron transfer
Electronic shuttle protein
Geological event
WWTPs

ABSTRACT

Anaerobic ammonium-oxidation (anammox) is a typical redox reaction driven by membrane electron transformation. However, the electron transfer mechanism of the core redox reaction and its evolutionary origins are still not thoroughly identified. In this study, a preliminary analysis was conducted for such interaction based on the 64 anammox bacterial genomes representing 12 genera available currently. The results suggested that enzymes involved in anammox reaction share the similar catalytic and electron transfer modes in different lineages, while the electron-carrying proteins shuttled between membrane and soluble enzymes are very different. A comparatively simple electronic shuttle protein system was encoded in the early-branching groundwater lineages Candidatus (Ca.) Avalokitesvara and *Ca.* Tripitaka, which was replaced by a sophisticated electron carrier scheme in the late-branching marine and terrestrial groups within family *Ca.* Brocadiaceae. Remarkably, the increasing availability of nitrite after Great Oxidation Event (GOE) potentially drove the adaptive evolution of the core redox systems by successively recruiting the nitrite reductase (NIR) for nitrite balance, a stable complex of two small cytochrome *c* proteins (NaxL and NaxS homologues) for electron transfer to HZS, as well as optimizing the structure of nitrite oxidoreductase gamma (NxrC) for electron conservation. In particular, a tubule-inducing nitrite oxidoreductase subunit (NxrT homologue) was further formed for electron transformation after the Neoproterozoic Oxygenation Event (NOE). Finally, based on two full-scale anammox-based wastewater treatment systems (WWTPs), we identified core gene transcriptional activities affecting the abundance of the family Ca. Brocadiaceae and their association with environmental factors. Overall, our study not only provides key information for understanding the dynamic patterns and evolutionary mechanisms of the anammox reactions and the associated electron transfers in conjunction with major geological events, but also provides new insights for future enrichment and effective applications.

1. Introduction

Highly metabolically diverse microorganisms, including ammonia-oxidizing bacteria (AOB)/archaea (AOA), nitrate-oxidizing bacteria (NOB), denitrifying bacteria, and anaerobic ammonium oxidation (anammox) bacteria, play a crucial role in the nitrogen cycles of both natural and human-made ecosystems (Kartal and Keltjens 2016; Rockström et al., 2009). Comparatively, no aeration requirements and greenhouse gas, such as nitrous oxide (N_2O), emissions have endowed anammox with significant cost-saving advantages, positioning it as the most promising biological N removal method (Kuenen 2020; Zhang et al. 2019) and has been estimated to contribute 30–70 % to the annual release of N_2 into the atmosphere (Kartal and Keltjens 2016). Several anammox reaction processes, such as partial nitrification-ammonia oxidation (PN/AMX), partial denitrification-ammonia oxidation (PD/AMX), simultaneous nitrification, ammonia oxidation, and denitrification (SNAD), as well as partial nitrification, ammonia oxidation, and methane-dependent nitrite/nitrate reduction (PNAM), are widely

* Corresponding authors at: Environmental Science and Engineering Research Group, Guangdong Technion-Israel Institute of Technology, 241 Daxue Road, Shantou, Guangdong 515063, PR China.
E-mail addresses: jidong.gu@gtiit.edu.cn (J.-D. Gu), yangych55@mail.sysu.edu.cn (Y. Yang).

https://doi.org/10.1016/j.watres.2025.123551
Received 2 January 2025; Received in revised form 4 March 2025; Accepted 24 March 2025
Available online 25 March 2025

applied in wastewater treatment (Liu et al. 2021; Zhuang et al. 2022). To date, the heterogeneous phylogenetic branches of anammox bacteria are composed of 12 genera, including *Candidatus* (*Ca.*) Brocadia, *Ca.* Jettenia, *Ca.* Kuenenia, *Ca.* Scalindua, *Ca.* Anammoxoglobus (Rich et al. 2020; Schmid et al. 2003; van de Vossenberg et al. 2013), as well as the newly identified *Ca.* Bathyanammoxibius, *Ca.* Loosdrechtia, *Ca.* Wujingus, *Ca.* Wunengus, *Ca.* Avalokitesvara, *Ca.* Tripitaka, *Ca.* Wukongus (Wu et al. 2023; Yang et al. 2022; Zhao et al. 2022).

The core anammox reaction is catalyzed by a series of redox-active enzymes, including hydrazine synthase (HZS), hydrazine dehydrogenase (HDH), nitrite oxidoreductase (NXR), hydroxylamine oxidase (HOX), hydroxylamine oxidoreductase (HAO)-like protein Kustc0458 (KsHN*, Ks represents *Kuenenia stuttgartiensis*, H represents HAO paralogues, N represent nitrite reduction, and * represents homologues) and nitrite reductase (NIR) (Kuenen 2008; Kuenen 2020). Core anammox enzymes distribute in a membrane-enclosed cellular compartment, anammoxosome (Akram et al. 2021; Almeida et al. 2015; Kartal and Keltjens 2016), and electrons are proposed to be shuttled between soluble and membrane enzyme complexes by electronic shuttle carriers, such as small c-type cytochromes (Akram et al. 2021; Akram et al. 2019b; Dietl et al. 2019). Nitrite (NO_2^-) reduction to nitric oxide (NO) catalyzed by NIR (Kuypers et al. 2018) or KsHN* (Ferousi et al. 2021; Maalcke et al. 2014; Okubo et al. 2020) coupled with a single-electron transfer, but the mechanism on electron shuttling between NIR/KsHN analog and membrane electron transport chain (ETC) is still unclear. Three electrons are consumed by HZS in transforming the produced NO and NH_4^+ to hydrazine (N_2H_4) (Kuenen 2008; Subba Rao et al. 2017). In the model anammox bacterium *Kuenenia stuttgartiensis*, two potentially electron carriers, kuste2854 (KsTH, TH represents tetraheme, a c554 family protein) (Ferousi et al. 2019) and NaxLS (Akram et al. 2019b) were identified. KsTH and its auxiliary proteins (kuste2855, kuste2856) are parts of the HZS cluster, potentially inducing direct interaction between the ETC electron transfer module with HZS (Ferousi et al. 2019). The lower redox potential (−175 mV) of NaxLS makes electron transfer from NaxLS to HZS more energy-efficient (Akram et al. 2019b). N_2H_4 is ultimately transformed to N_2 (Kuenen 2008) catalyzing by HDH at extremely low redox potentials with the release of four electrons (Kuenen 2008), which are preferentially transferred to the ETC to drive the quinone cycle and ATP biosynthesis (Akram et al. 2019a; de Almeida et al. 2016; Kartal et al. 2011b). Additionally, hydroxylamine (NH_2OH), a byproduct of N_2H_4 synthesis could escape from HZS and inhibit the activity of HDH (Kartal et al. 2011a). It could be further oxidized to NO through a three-electron reaction catalyzed by HOX (Kuenen 2008; Kuenen 2020). The existing result suggested that Kustc0563 is a promising redox partner of HOX for the transferring of the three released electron from NH_2OH oxidation in *Kuenenia stuttgartiensis* (Akram et al. 2021). It was proposed that the two electrons released from NO_2^- oxidation to nitrate (NO_3^-) catalyzed by NXR could be further transferred to NIR or KsHN* for NO_2^- reduction rather than the previously believed CO_2 fixation (Chicano et al. 2021; Hu et al. 2019), in which NxrT was characterized as an electron transfer shuttle protein (Chicano et al. 2021).

However, the generalizability of the core anammox reaction and the associated electron-transfer mechanisms explored in *Kuenenia stuttgartiensis* is reasonably questioned due to the such high diversity of anammox bacteria (Wu et al. 2023; Yang et al. 2022; Zhao et al. 2022). Here, we systematically analyzed the potential models of electron transfer in anammox metabolism based on the up-to-date 64 high-quality anammox bacterial genomes affiliated to 12 different genera. Interactions between key anammox enzymes and the corresponding redox chaperones were systematically investigated in diverse lineages. The ongoing evolutionary process of the electron transport mechanisms in anammox bacterial community in conjunction with major geological events was further analyzed. The core anammox-reactive enzymes with species abundance and environmental factors were analyzed in two full-scale anammox-based wastewater treatment systems (WWTPs). The detailed elaboration of core redox reactions and their associated electron transfer mechanisms provide new insights into the adaptive evolution of anammox bacteria.

2. Materials and methods

2.1. Anammox bacterial genome annotation

In total, 64 anammox bacterial genomes representing 12 genera were downloaded from NCBI (Table S1). The quality of obtained genomes was initially evaluated using the module "lineage_wf" of CheckM v1.0.6 (Parks et al. 2015). Open reading frames (ORFs) were predicated from these genomes using Prodigal v2.6.3 using the "- p single" option (Hyatt et al. 2010). Predicted ORFs were annotated by BLAST+ v2.9.0 searches against a previously constructed custom nitrogen cycle database (Yang et al. 2022) with the standard requirements of E-value $\langle 10e^{-10}$, amino acid identities $\rangle$ 30 %, and a minimum alignment length $>$ 50 %. We further filtered the candidate sequences based on conserved regions identified by PyMOL v 2.3.2 with "pymol.cmd.align" and default setting (Yuan et al. 2016). To obtain the amino acid sequence of potential electron transfer shuttle proteins, we constructed a custom database, composing the identified KsTH from *Ca.* Kuenenia stuttgartiensis (Ferousi et al. 2019), NaxLS from *Ca.* Kuenenia stuttgartiensis (Akram et al. 2019b) and *Ca.* Jettenia *caeni* (Ukita et al. 2010), Kustc0563 from *Ca.* Kuenenia stuttgartiensis (Akram et al. 2021), NxrT from *Ca.* Kuenenia stuttgartiensis (Chicano et al. 2021). Subsequently, predicted ORFs were analyzed by BLASTP searches against a custom database with the requirements of E-value $\langle 10e^{-10}$, amino acid identities $\rangle$ 30 %, and conserved regions identified by PyMOL v 2.3.2 with "pymol.cmd.align" and default setting (Yuan et al. 2016) were also used to select retained sequences.

2.2. Protein architecture construction and validation

Well-characterized protein structures of core anammox enzymes, including HZS (PDB: 5c2v, *Ca.* Kuenenia stuttgartiensis), NaxLS* (PDB: 6R6 M, *Ca.* Kuenenia stuttgartiensis), NirK (PDB: 5zli, *Ca.* Jettenia) and HOX (PDB: 4n4k, *Ca.* Kuenenia stuttgartiensis) were downloaded from PDB database for downstream analysis. Due to the absence of available structures of NirS and KsTH* in anammox bacteria, we used Alpha-fold2 for their structure model prediction. Specifically, the NirS and KsTH protein sequences were extracted from *Ca.* Kuenenia sp. isolate AMX1, and Alpha-fold2 was configured with parameters mas_mod= "mmseqs2_uniref_env", pair_mod="unpaired_pair", model_type="auto", num_recycles=30 (Mirdita et al. 2022). Model predictions are initially evaluated based on sequence coverage and pLDDT (Mirdita et al. 2022). And, the constructed model also was further evaluated by SAVES v6.0 (Colovos and Yeates 1993; Pontius et al. 1996). Visualization and retouching of the model were carried out by PyMOL v 2.3.2 (Yuan et al. 2016).

2.3. Interaction analysis

The interaction analysis of hydroxylamine (NH_2OH) and HOX was performed according to Maalcke WJ, et al. (Maalcke et al. 2014), and the protein interaction between kustc0563 and HOX was carried out following Akram M, et al. (Akram et al. 2021). Also, the surface analysis of protein interaction between NaxLS* and HZS was carried out by Z-dock (Pierce et al. 2014) and PDBePISA (https://www.ebi.ac.uk/pdbe/pisa/) with the default settings. To compare structure differences of NirK and NirS between anammox bacteria and denitrifying bacteria, some typical NirK (PDB: 3ZIY, *Ralstonia pickettii* 12 J; PDB: 6hbe, *Thermus scotoductus* SA-01) and NirS (PDB: 1nir, *Pseudomonas aeruginosa*) were downloaded from PDB database. The predicted NirS in *Ca.* Kuenenia sp. isolate AMX1 and NirS from *Pseudomonas aeruginosa* were entered into PyMOL v 2.3.2 (Yuan et al. 2016), and the two proteins

were compared using "pymol.cmd.align" with the parameters set to cycles=10 and default. Amino acid residues centered on the two hemes were then displayed within a range of 4A for further comparison.

2.4. Phylogenetic analysis

The 43 concatenated marker genes were identified from the all retained anammox bacterial genome produced by Check M v1.0.6 "lineage_wf" module with the default setting (Parks et al. 2015) for phylogenetic analysis. Alignment gaps were removed using trimAl V2.0 with the setting '-gt 0.1′ (Capella-Gutiérrez et al. 2009), and the maximum likelihood tree of the 43 concatenated marker genes was constructed using IQ-TREE2 V1.6.12 (Minh et al. 2020) with the best-fit model JTTDCMut+F + R4 selected by ModelFinder (Kalyaanamoorthy et al. 2017).

Similarly, for the phylogenies of NaxL* and NaxS* sequences. The closely relative reference sequences of NaxL* and NaxS* in the NCBI nr database were identified by BLASTp (Mahram and Herbordt 2015) using these sequences extracted from anammox bacterial genomes as the queries and the E-value of $10e^{-10}$, reference sequences with amino acid identities > 50 % were selected. The NxrT* sequences recovered from anammox bacterial genomes were used as a queries in BLAST+ v2.9.0 search (Mahram and Herbordt 2015) against the NCBI nr database. Since the consistency of NxrT* is quite low among different anammox bacterial lineages, we set the blast threshold as E-value ⟨ $10e^{-10}$, amino acid identities ⟩ 20 %, a minimum alignment length > 50 %, and the presence of conserved regions was used to filter the reference NxrT* sequences. The candidate sequences of NaxL*, NaxS*, and NxrT* were aligned using MAFFT v7.463 (Katoh et al. 2002) and gaps in alignment were removed using trimAl V2.0 with the setting '-gt 0.1′ (Capella-Gutiérrez et al. 2009). Maximum likelihood trees of NaxL*, NaxS* NxrT* were constructed using IQ-TREE2 V1.6.12 (Minh et al. 2020) with 1000 ultrafast bootstraps and Dayhoff+F + I + G4, Dayhoff+G4, and JTT+F + I + G4 substitution models, respectively. The built trees were visualized and modified using iTOL v7 (Letunic and Bork 2021).

2.5. Sequence complementary analysis

Sequence alignment of targeted HZS, NxrC, HOX, NIR, KsTH*, NaxLS*, and NxrT* in various anammox bacteria were produced by MEGA version11 (Tamura et al. 2021) and comparison of predicted and analyzed structure was carried by PyMOL align module with "pymol.cmd.align" model and default settings. Display for the alignment was generated using the GeneDoc (https://github.com/karlnicholas/GeneDoc. Version 2.7). The core gene locus in anammox bacteria genomes were produced in GeneSpy (Garcia et al. 2019) by centering on the NXR.

2.6. Transcriptome and correlation analysis of two full-scale anammox-based wastewater treatment plants (WWTPs)

To explore the core redox reaction key enzymes in the wastewater lineage *Ca*. Brocadiaceae in practical applications, we analyzed two full-scale anammox-based wastewater treatment systems in Guangzhou and Germany, which including *Ca*. Brocadia, *Ca.* Jettenia, *Ca*. Kuenenia and *Ca*. Loosdrechtia (Hu et al. 2023; Yang et al. 2021). Raw reads of metagenomic were quality controlled by MetaWRAP read_qc and default setting (Uritskiy et al. 2018). Then, the retained clean reads were *de novo* assembled by MEGAHIT V1.1.4 (–k-min 23 –k-max 141 –k-step 20) (Li et al. 2015), metagenome-assembled genomes (MAGs) obtained was carried out by metabat2, maxbin2, concoct, and refined by MetaWRAP bin_refinement with the parameter "-c 50 -x 10″ (Uritskiy et al. 2018). Ribosomal RNA (rRNA) reads were first removed from the raw transcriptome data using SortMeRNA (version 2.1) to construct non-rRNA read libraries (Kopylova et al. 2012) based on the SILVA 132 database. All MAGs abundance (TPM) of DNA and cDNA transcript were calculated by CoverM (https://github.com/wwood/CoverM) "genome" and "contig" module, and Transcript abundance is further normalized by genomic abundance. Pearson's correlation coefficients between the genes abundance, factors and anammox bacteria abundance matrices was constructed using the "Hmisc" package in R (Varsadiya et al. 2021). We then applied the false discovery rate (FDR) controlling procedure to calculate *p*-values for multiple testing (Benjamini and Hochberg 2018).

2.7. Data available

All anammox bacteria genome were deposited at NCBI GenBank database, the accession number are described in Table S1. Raw metagenomic and metatranscriptomic data of two WWTPs have been deposited into NCBI under the BioProject PRJNA526440 and PRJNA815463.

3. Results and discussion

3.1. Conserved anammox reactions and the related electron transformation systems

The generated NO by NO_2^- reduction catalyzed by NIR is a precursor for N_2H_4 formation, and thus this reaction is considered a key step in anammox metabolism (Fig. 1) (Dietl et al. 2019; Ferousi et al. 2021; Hira et al. 2012). In detail, cytochrome *cd1* nitrite reductase (NirS) is commonly encoded by *Ca.* Kuenenia and *Ca.* Scalindua, which is replaced by a copper-containing nitrite reductase (NirK) in *Ca.* Jettenia (Hira et al. 2012), *Ca.* Wujingus and *Ca.* Loosdrechtia (Fig. 1). Comparatively, only a few *Ca*. Brocadia species possess the coding regions for NirK and NirS (Fig. 1) (Gori et al. 2011; Okubo et al. 2020; Palomo et al. 2022). The high sequence identities of NirS (≥74 %) and NirK (≥ 67 %) across various lineages likely indicate that they share similar catalytic capabilities among anammox bacteria (Table S3). The predicted architecture assessment of the NirS in "*Ca.* Kuenenia sp. isolate AMX1" (Fig. 2a) indicates that NirS has a highly reliable protein topology structure (80.7 % plausible amino acid residue regions, 83.4 % pLDDT, and 0.798 pTM) (Mirdita et al. 2022). Subsequently, structure alignment between *Pseudomonas aeruginosa* (PDB: 1nir) and "*Ca.* Kuenenia sp. isolate AMX1" NirS sequences suggested they share a high similarity in the value of root-mean-square deviation (RSMD, 0.785), and two heme-centered amino acid residues in the range 4A (Fig. 2d). According to the well-established catalytic and heme-binding sites of NirS in *Pseudomonas aeruginosa* (PDB: 1nir), we proposed that *c*-heme and d_1-heme are the electron entry site and catalytic site in anammox bacterial NirS, respectively (Fig. 2d) (Klünemann and Blankenfeldt 2020; Nurizzo et al. 1997). NirK encoded by anammox bacteria is a tetramer enzyme containing three different copper centers, Cu1c: C-terminus type 1 Cu, $Cu1_N$: N-terminal type 1 Cu, and Cu2: N-terminal type 2 Cu (Fig. 2a and b). Type III NirK has also been found in *Thermus scotoductus* SA-01 (PDB: 6hbe, Fig. S2c) (Opperman et al. 2019). Compared to dicopper NirK, a special sensing loop was found in tricopper NirK for electron transport between $Cu1_N$ and Cu2 when NO_2^- binding to CuII (Opperman et al. 2019). Consistently, these coding regions were also found in anammox bacterial NirK for electron transformation (Fig. S2d). Fig. 2e illustrates the profile of the different mechanisms by which electron transfer occurs during the NO_2^- reduction catalyzed by NirK and NirS. In NirK, Cu1c firstly admits electrons discharged from the ETC or NxrT*, which are then transferred to Cu2 via Cu1N and the sensing loop to mediate the reduction of NO_2^-. In NirS, heme c receives exogenous electrons, which are subsequently transferred to the catalytic center, heme d_1, for NO_2^- reduction.

Alignment of HZS sequences retained from all anammox bacterial genomes revealed that HZS is a highly conserved oxidoreductase (Fig. S1d, f and h) as suggested by previous studies (de Almeida et al. 2016; Dietl et al. 2015; Kuypers et al. 2018). HZS is a crescent-shaped dimer of heterotrimer ($\alpha_2\beta_2\gamma_2$) (Fig. 1a), in which the α- and

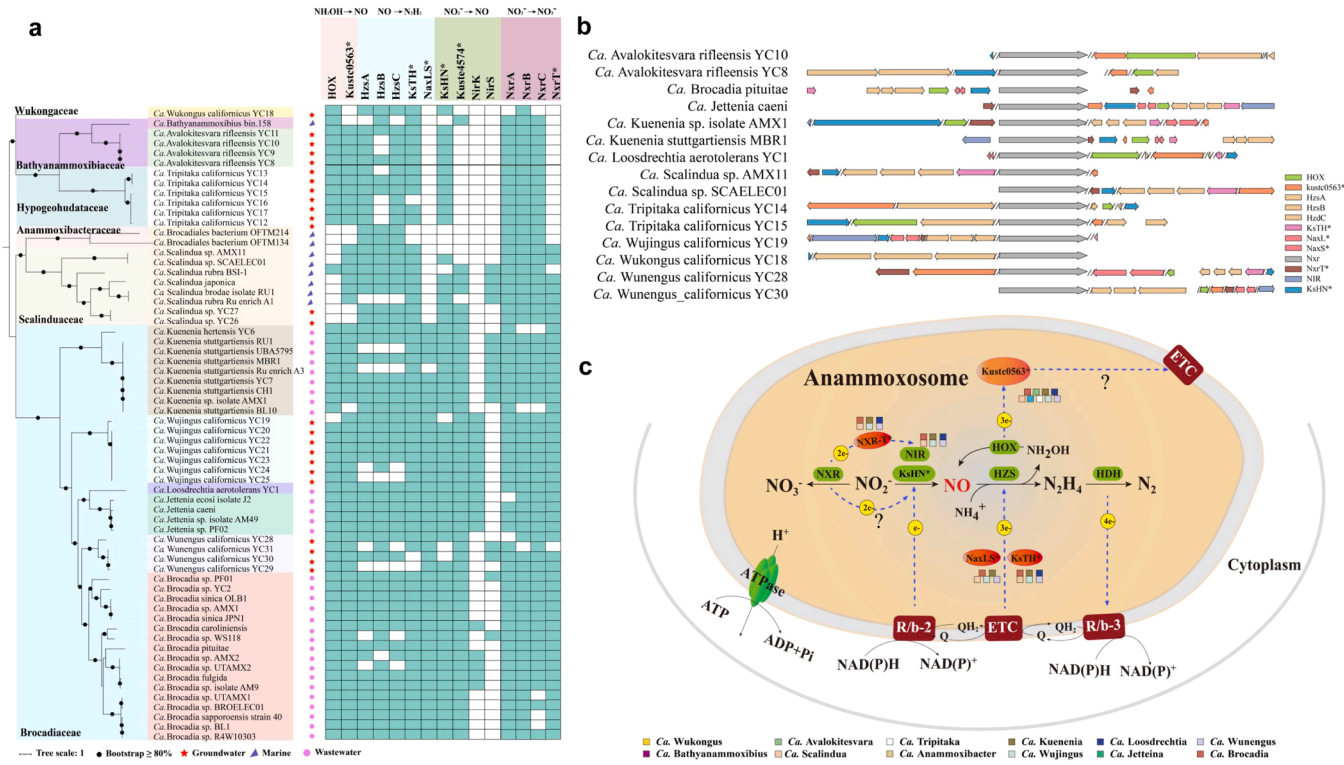

Fig. 1. The constructed overall anammox metabolism and the associated electron transformation pathways. (a) Phylogenetic analysis of the 64 anammox bacteria genomes and presence of anammox related functional genes based on 43 concatenated markers gene, gene data were deposited in Table S2 and S3. (b) Gene locus of core anammox enzymes centered on NXR and sequence arrangements in represent anammox bacteria genomes, (c) Re-construction of core anammox reactions and the associated electron transformation pathways. NXR/Nxr, nitrite oxidoreductase; NIR, nitrite reductase; HZS, hydrazine synthase, α-subunit (HzsA), β-subunit (HzsC), γ-subunit (HzsB); HOX, hydroxylamine oxidase; HDH, hydrazine dehydrogenase; NxrT*, tubule-inducing NXR subunit; KsHN*, NO: nitrite oxidoreductase (kustc0458 paralogues), Ks represent *Kuenenia stuttgartiensis*, H represent HAO paralogues and N represent nitrite reductase; KsTH*, a c554 tetraheme protein, Ks represents *Kuenenia stuttgartiensi*, TH represents tetraheme; NaxLS*, class I and class II c-type cytochromes; ETC, membrane electron transport chain in anammoxosome; *, paralogues of various enzymes.

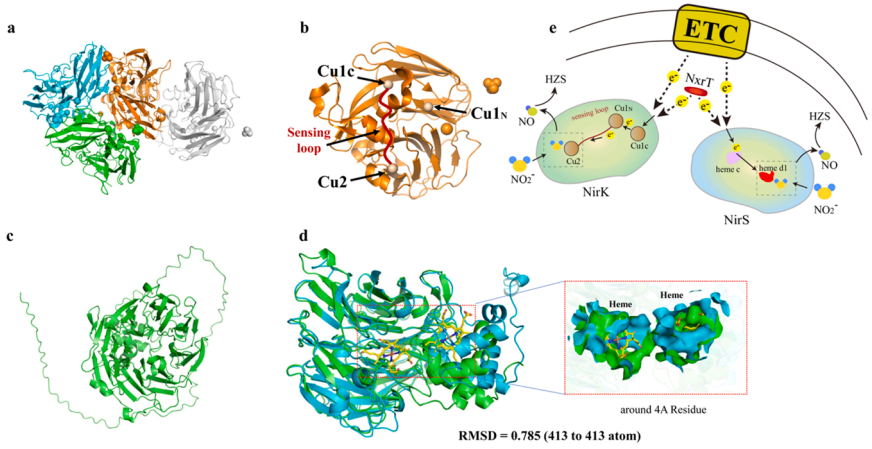

Fig. 2. Protein architectures and working outlines of NirK and NirS related to nitrite reduction in anammox bacteria. Architectures of NirK (a) and copper ion distribution in NirK (b) in *Ca.* Jettenia caeni (PDB: 5ZL1). Alpha-fold2 predicted NirS structure in *Ca.* Kuenenia sp. Isolate AMX1 (CAADGZ010000145.1_3) (c) and protein align analysis with well-characterized NirS structure in *Pseudomonas aeruginosa* (PDB: 1NIR) (d). Working outline of NIR in anammox bacteria (e). $Cu1_C$, C-terminus type 1 Cu; $Cu1_N$, N-terminal type 1 Cu; Cu2, N-terminal type 2 Cu.

γ-subunits contain two hemes, and calcium (Ca) and zinc (Zn) ions are spread across the three subunits (Fig. 1b, c, e and g) (Dietl et al. 2015). Comparative alignment analysis determined that the substitution of tyrosine (Tyr) for histidine (His) in the α-subunit of the C-type heme-binding motif cysteine (Cys)- His (CxxCH) is conserved as a potential active site (Fig. S1d) (Kim et al. 2012). Meanwhile, a loop ring composed by 15 amino acids in β subunit (β245–260) (Kim et al. 2012) was also identified in all retained HZS (Fig. S1g and h). Binding hemes γI and γII in the γ-subunit (Kim et al. 2012) with conserved sites for receiving external electrons (Fig. S1e and f) and histidine as a potential catalytic redox amino acid in the γ-subunit also were recovered in all obtained HZS sequences (Fig. S1f and h). Therefore, we conclude that the HZS enzymes endocatalytic and the associated electron transfer pathways are conserved in all the currently known anammox bacterial

lineages (Fig. 3b).

HOX catalyzes the three-electron reaction of NH_2OH to NO, is another characteristic enzyme in anammox bacteria(Ferousi et al. 2019; Kartal and Keltjens 2016) (Figs. 1 and 2d). A total of 55 HOX coding amino acid sequences were identified from anammox bacteria. Interestingly, although HOX sequences were divided into two clades in the phylogenetic tree (Fig. S3a), the structures of the eight circularly arranged hemes were highly conserved (Fig. S3b) (Fernández et al. 2008; Maalcke et al. 2014). This result suggests all anammox bacteria encode a similar electron transfer pathway in HOX. Additionally, NH_2OH binding and catalytic sites are also identical based on docking and sequence alignment analysis (Figs. 4b and S3d) (Maalcke et al. 2014). Interestingly, unlike the hydroxylamine oxidoreductase in *Nitrosomonas europaea* (NeHAO), HOX catalyzes the oxidation of NH_2OH terminating in NO. one plausible reason is that Tyr at position 358 in NeHAO provides a hydrophilic hydroxyl group (Cedervall et al. 2013; Igarashi et al. 1997; Maalcke et al. 2014), while methionine (Met) at position 323 in HOX is a hydrophobic amino acid, which prevents water molecules in the cavity from attacking the substrate bound to the P460 heme, thereby stop the reaction of NO to NO_2^- (Maalcke et al. 2014). Differently, the N-terminal structural domain of HOX likely associated with NeHAO, presents a strong negative charge (Maalcke et al. 2014), is not fully conserved in early- and late-branching lineages. In the N-term of late-branching, such as *Ca.* Brocadia, *Ca.* Jettenia, *Ca.* Wujingus, the positively charged lysine (K) in the early-branching *Ca.* Avalokitesvara and *Ca.* Tripitaka was replaced by a negatively charged glutamic acid (E) or an uncharged asparagine (N). Again, the starting amino acid threonine (T) of the N-term was lost in *Ca.* Avalokitesvara (Fig. S3c). Unfortunately, the lack of structural and functional analysis of the N-term in HOX blocks the accurate assessment of the consequences of these site mutations.

NxrA, NxrB, and NxrC sequences of the late-branching lineages of anammox bacteria share relatively high identities (> 60 %) (Table S4), while NxrC have much low identities with those of early-evolved groundwater groups *Ca.* Avalokitesvara (31–35 %) and *Ca.* Tripitaka (37–38 %) (Table S4). Sequence complementary spectrum revealed that the heme b binding site in NxrC is conserved in all anammox bacteria (Fig. S6a), except for the replacement of methionine (Met, M) by arginine (^{372}Arg, R) in *Ca.* Avalokitesvara. Met has only one sulfur group bound to heme b in the side chain (Li et al. 2011), while the positive charge and special groups (amino and carboxyl groups) in Arg can form charge complementary (Armstrong et al. 2016; Sarkar et al. 2023) and *van der Waals* interactions (Astashkin et al. 2012) with heme b, increasing the binding strength. Interestingly, the NxrC coding regions of the early-branching *Ca.* Avalokitesvara and *Ca.* Tripitaka also contain two classic type-c heme-binding motif CxxCH (Li et al. 2011). According to the function of the similar structure in HAO homolog, the heme bound by CxxCH is believed to have the potential to conserve more electrons (Maalcke et al. 2014). The early anammox bacteria diverged around 1.52 Ga (Table S1) predominantly inhabited groundwater ecosystems

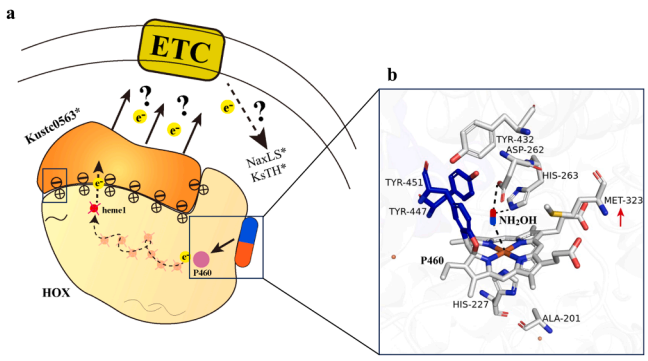

Fig. 4. Potentially working outline of HOX. HOX catalysis and Kustc0563*-mediated electron transfer (a) and docking analysis of NH_2OH with HOX (b) in *Kuenenia stuttgartiensis*. TYR: Tyrosine, HIS: Histidine, ALA: Alanine, ASP: Aspartic acid, MET: Methionine, Numbers indicate amino acid sites. *, paralogues of various enzymes.

(Fig. 1a) with quite low substrate availability due to the diffusion bottlenecks for NO_x^- and NH_4^+ (Aeschbach-Hertig and Gleeson 2012) (Ağca et al. 2014; Spalding et al. 2019). To adapt to this ecological niche, *Ca.* Avalokitesvara and *Ca.* Tripitaka initiated a "self-protection" mechanism by conserving additional electrons by the heme bound by CxxCH. NXR has also been found to have the potential to catalyze the reverse reaction by reducing NO_3^- back to NO_2^- (Chicano et al. 2021). The conserved electrons could be used to reduce NO_3^- by the reversable NXR to enlarge the substrate acquisition pathway. Conversely, the late-branching marine *Ca.* Anammoxibacteraceae and *Ca.* Scalinduaceae (1.35 Ga) and terrestrial *Ca.* Brocadiaceae (0.99 Ga) (Table S1, Fig. 6) could acquire more substrate in the oxidized surface of the Earth compared to the subsurface (Stüeken et al. 2016; Stüeken et al. 2024). Meanwhile, late-evloved branching lineages have higher conservation of NxrA, NxrB and NxrC (Table S4), NxrC electron-conserving sites that evolved as result of substrate limitation were discarded (Fig. 5).

3.2. *Auxiliary shuttle proteins and taxonomically dependent electron transfer models in anammox metabolism*

Three-electron transfer between anammoxosome membrane and HZS is the rate-limiting step for N_2H_4 synthesis (Almeida et al., 2015), and KsTH* or soluble electron carriers NaxLS* were proposed to aid the electron transfer (Arp et al. 2007; Ferousi et al. 2019). The conserved Cys-lysine (Lys)-Cys-His (CKCH) heme-binding motif and four hexa-coordinate hemes with low spin, including His/Lys (heme 1), His/Cys (heme 2), and two His/His connections (heme 3 and heme 4), were also observed in the identified KsTH* proteins in anammox bacterial genomes (Fig. S4) (Ferousi et al. 2019). NaxLS* encoding sequences were also obtained with the heme-binding motifs in NaxL* and

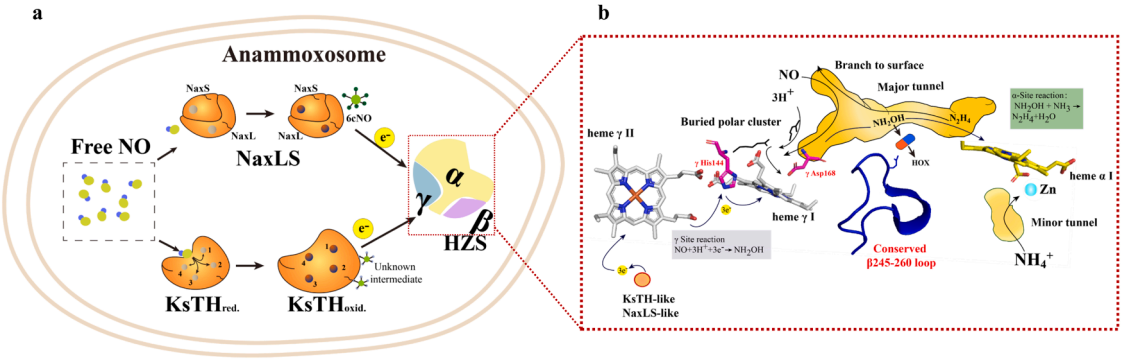

Fig. 3. Working mechanisms of NO conversion to N2H4. Workflow of the electron shuttle proteins NaxLS and KsTH (a) and mechanism of HZS-catalyzed N_2H_4 synthesis (b). red., reduction state; oxid., oxidation state. The operational mechanism of HZS shown in Panel b was constructed based on (Kartal and Keltjens 2016).

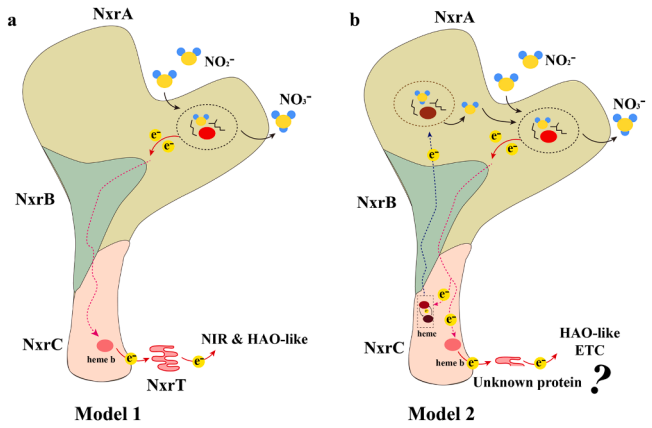

Fig. 5. Two potential modes of NXR catalysis and electron transfer mechanism. Schematic diagram of catalysis and electron transfer after NxrT recruitment (a), schematic diagram of catalysis and electron transfer before NxrT recruitment (b).

NaxS* subunits (Fig. S5). Interestingly, KsTH* and HzsABC belong to the same gene cluster and are also commonly encoded by distinct anammox bacteria (Fig. 1a and c). Differently, NaxLS* is deficient in the early-branching *Ca.* Anammoxibacter, *Ca.* Avalokitesvara, and *Ca.* Tripitaka as well as marine *Ca.* Scalindua and *Ca.* Bathyanammoxibius (Fig. 1a, Table S1). By expanding the sequence analysis beyond NaxLS* protein in anammox bacteria, it was found that NaxLS* protein is only obtained in *Planctomycetes* under the condition of 60 % identity as standard, suggesting a potential gene transfer at the later stage (Fig. S5a and b). Existing studies suggested that KsTH*enables electron transfer between different modules through interactions with quinones on the membrane of the anammoxsome or through direct contact with HZS (Akram et al. 2021; Kartal and Keltjens 2016), but the working mechanism is still unclear. Here, molecular interaction between NaxLS* and HZS from *Kuenenia stuttgartiensi* was analyzed to explore the underlying mechanism. The result showed that the heme-binding region of NaxL* had a stronger interaction with HZS compared to the heme-binding motif of NaxS* (Table S5). In particular, the heme-binding region in γ subunit interacts strongly with NaxL* (Table S5), which is consistent with the finding that γ subunit is the subunit involved in electron transfer in the HZS (Kim et al. 2012). Additionally, γHis^{144} involved in the catalytic redox reaction also formed hydrogen bonds with NaxL (Table S5). Unexpectedly, NaxS* had no interaction with α and γ subunits (Table S5), but showed a specific interaction with β subunit of HZS, which is composed of seven β propeller blades (Fig. S1g) (Dietl et al. 2015). The β propeller blades are believed to involve in protein-protein interactions and cofactors bindings that guide the activities of various enzymes, such as NirS, NO reductase, methanol and methylamine dehydrogenase (Afanasieva et al. 2019; Chen et al. 2011). Conclusively, the working scheme of electron shuttle protein and HZS in anammox bacteria was proposed (Fig. 3). NO was captured by NaxLS* and/or KsTH* and form a 6cNO (Ukita et al. 2010) and an unknown intermediate (Ferousi et al. 2019; Zhang et al. 2019), this reaction facilitates the electron retention of the heme conversion in the redox reactions, followed by a strong interaction of NaxLS* and KsTH* with HZS for electron transformation.

NH_2OH oxidation is accompanied by the release of three electrons (Akram et al. 2021; Maalcke et al. 2014), which are likely transferred to HZS via ETC and small c-type cytochromes kustc0563* (Akram et al. 2021). Kustc0563*, the redox partner of HOX, was encoded by all anammox bacteria, indicating the kustc0563*-mediated three-electron transfer mechanism is conserved. The conserved complementary charge interactions of kustc0563* with HOX surface residues site suggest the tight anchoring between them for electron transformation (Figs. 4 and S9). Both heme 1 and heme 3 locate near the interaction region of HOX, while only heme 1 exposes to the solvent (Akram et al. 2021), that the generated three electrons by HOX should be released via heme 1 (Fig. 4b). Unfortunately, the acceptors of these three electrons are still unknown. Indeed, The HOX responsible for NH_2OH oxidation is a soluble multiheme c-type cytochrome complex that is not spatially associated with the anammoxosome membrane (Kartal and Keltjens 2016; Maalcke et al. 2014), and due to the high specificity of the electron shuttling system, the low-potential electrons (−30 mV) released by HOX should at least be preferentially transported to the ETC to prevent the system from effectively short-circuiting (Akram et al. 2019a; Maalcke et al. 2014). Additionally, in *Nitrosomonas europaea,* the turnover of NeHAO produces four electrons that are transferred to the electron transfer protein cytochrome c554 (Cyt c554, similar to Kustc0563* (Akram et al. 2021)), and two of the product electrons can be transferred back to the AMO by Cyt c554 for ammonia oxidation (Cedervall et al. 2013). Because HOX and NeHAO share a common protein architecture, structurally similar P460 co-factors, NH_2OH catalytic site and auxiliary electron shuttle protein (Maalcke et al. 2014), we hypothesize that the electrons released by HOX may also return to the HZS with the substrate similarly to NeHAO. In summary, the leaked NH_2OH during N_2H_4 synthesis is further oxidized to NO by HOX, and the generated three electrons are transferred to the anchoring protein kustc0563* through the 8 ring-arranged hemes in HOX, then kustc0563* dissociates from HOX and transfers electrons to the HZS via ETC (Fig. 4a).

The oxidation of NO_2^- to NO_3^- catalyzed by NXR is accompanied by the release of two electrons, which has been believed to be used for CO_2 fixation (de Almeida et al. 2016). Recent studies indicate that these two electrons were transferred to nitrite reductase (NIR or KsHN*) for the NO_2^-reduction, as *Kuenenia stuttgartiensis* could fix CO_2 in the absence of NO_2^- (Chicano et al. 2021; Hu et al. 2019). NxrT* in *Kuenenia stuttgartiensis* was proposed as an electron transfer shuttle protein between NXR and nitrite reductase (Chicano et al. 2021). It was encoded by all known anammox bacteria only except for the early-branching *Ca.* Avalokitesvara and *Ca.* Tripitaka (Table S4, Fig. S6b), suggesting the early anammox bacteria cannot directly use the generated electrons by NXR for NO_2^-reduction or handle the electron transfer by an unidentified ancient shuttle system. NxrT* and NirK/NirS were simultaneously acquired by the late-branching anammox bacteria (Fig. 1a and c), likely indicating a strong connection between NxrT* and NIR in the anammox catabolism. Phylogenetic analysis divided NxrT* into three clades (Fig. S7), in which clade 2 is solely constituted by *Ca.* Kuenenia NxrT*. Clade 2 contains two distinct branches (Fig. S7), where the NxrT in branch 1 is cluster with the NXR gene (Fig. S7b, Table S5). In contrast, clade 1 and clade 3 NxrT* are present on distinct genetic locus as illustrated in a previous study (Chicano et al. 2021). The closest phylogenetic relationship of NxrT* between late-branching anammox bacteria and other *Planctomycetes* (Fig. S7) likely suggesting anammox bacteria acquire NxrT* through gene transfer from the ancestor of *Planctomycetes*.

3.3. *Evolutionary mechanisms of the core redox reaction system in conjunction with geological events*

The origin and divergence times of diverse anammox bacterial lineages has been investigated (data not shown, manuscript submitted), which showed that the earliest divergence time of the existing anammox bacteria was 1.52 Ga (Table S1), during the Mesoproterozoic era (1.6–0.8 Ga). The onset of the Great Oxygenation Event (GOE, ca. 2.4–2.3 Ga) marked the commencement of increased oxygen levels in Archaean Earth, which subsequently stimulated the accumulation of NO_3^- (Fig. 6) (Bekker and Holland 2012; Stüeken et al. 2016) and the divergency of anammox bacteria (Liao et al. 2022). Mesoproterozoic era is recognized as a pivotal period for the emergence of eukaryotes (Knoll and Nowak 2017) that the expansion of eukaryotic algae lead to the NO_3^- limitation in the ocean (Knoll and Nowak 2017; Stüeken et al. 2024; Tao et al. 2022). At the same time, the rise in atmospheric oxygen levels and

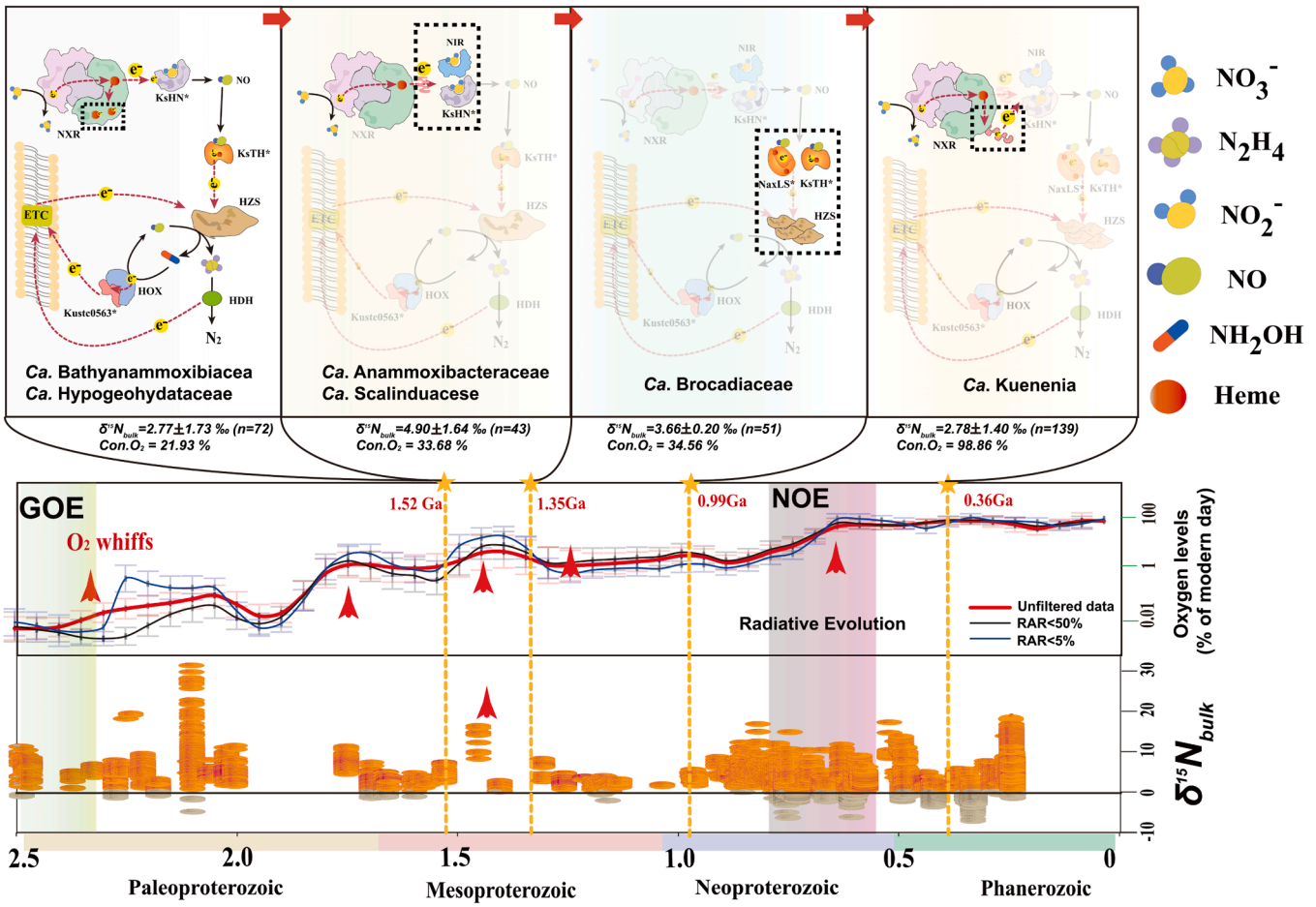

Fig. 6. Potentially evolutionary trajectories of various electron transfer systems in anammox bacteria in conjunction with major geological events. GOE, Great Oxidation Event; NOE, Neoproterozoic Oxygenation Event; KsTH*, KsTH homologues; KsHN*, Kustc0458 homologues; Kustc0563*, Kustc0563 homologues. $\delta^{15}N_{bulk}$ information was obtained from (Stüeken et al. 2024) and Table S6, oxygen level data was collected from (Chen et al. 2022).

the influx of sulfide fluxes into the oceans have resulted in the removal of essential metal ions, such as molybdenum and copper (Poulton et al. 2010; Tao et al. 2022). This depletion has consequently diminished the activity of nitrogen-fixing enzymes and contributed to a scarcity of NO_x^- in marine environments. Although NO_x^- generated by microbial oxidation of NH_4^+ on land provides a source of NO_3^- in the shallow oxygenated waters of the oceans, pervasive shortages of NO_x^- were characteristic of aquatic ecosystems on the Mesoproterozoic Earth (Stüeken et al. 2016; Stüeken et al. 2024; Tao et al. 2022; Wang et al. 2023a). The deficit of NO_x^- has constrained the pathway for KsHN-catalyzed conversion of NO_2^- to NO. To mitigate this challenge, the early clades *Ca.* Bathyanammoxibiaceae and *Ca.* Hypogeohudataceae have evolved to conserve two electrons by incorporating an additional heme group in NxrC (Fig. 6), which enables anammox bacteria to acquire more NO_2^- through NO_3^- reduction catabolized by the reversable NXR (Chicano et al. 2021) or ensure a sufficient electron supply for NO_2^- reduction catabolized by the KsHN. Simulations of $\delta^{15}N_{bulk}$ and oxygen concentrations indicate that oxygen fluctuations during the late Mesoproterozoic era (approximately 1.5–1.3 Ga) (Canfield et al. 2018; Chen et al. 2022; Stüeken et al. 2016) increased the NO_x^- availability in marine ecosystems (Stüeken et al. 2016; Tao et al. 2022) (Fig. 6). Consequently, marine *Ca.* Anammoxibacteraceae and *Ca.* Scalinduaceae have lost the two additional heme-binding sites in NxrC. Instead, NIR and NxrT* were recruited by marine anammox bacteria (Fig. 6). As described above, NxrT may translocate the two electrons released by NXR to KsHN, leading us to hypothesize that the recruitment of NxrT* probably enhance the reduction of NO_2^- to NO catalyzed by KsHN. NIR has been recognized as a critical enzyme for core redox anammox reactions (Gori et al. 2011; Kuypers et al. 2018; Schmid et al. 2003). However, its absence has been prevalent in the early anammox bacterial lineages, suggesting that the primary function of the NIR enzyme may be NO_2^-detoxification under the force of increasing NO_2^-, a notion consistent with earlier speculations (Yang et al. 2022; Yang et al. 2020). During the early Neoproterozoic, particularly prior to the Neoproterozoic Oxygenation Event (NOE), oxygen concentrations remained relatively stable (Chen et al. 2022) (Fig. 6). The low $\delta^{15}N_{bulk}$ values imply that fixed nitrogen in the water column may have been dominated by minimal levels of ammonium (Fig. 6). NO_3^- produced through nitrification may have been rapidly replaced by denitrification, preventing accumulation (Stüeken et al. 2024). In contrast to marine ecosystems, terrestrial weathering provided more NH_4^+ and NO_x^-(Horton 2015), allowing anammox bacteria (*Ca.* Brocadiaceae) to not only migrate from marine or groundwater environments to terrestrial ecosystems but also to adapt to a substrate-rich environment through the recruitment of NaxLS* and HZS multiple copy (Fig. 6). *Ca.* Kuenenia, which is affiliated to *Ca.* Brocadiaceae, diverged around 0.36 Ga (Table S4). Notably, in contrast to other members of *Ca.* Brocadiaceae, the NxrT enzymes of *Ca.* Kuenenia are classified into two types: free enzymes and those clustered with NXR (Figs. 1b, 6 and S6, Table S4). Indeed, following the NOE, the increase in oxygen levels and $\delta^{15}N_{bulk}$ values suggests a further enhancement of NO_x^- and NH_4^+ (Stüeken et al. 2024) (Fig. 6). However, this change does not appear to have influenced the anammox systems of other members of the *Ca.* Brocadiaceae family, indicating that there may be additional factors driving the evolution of *Ca.* Kuenenia. Previously

studies have demonstrated that *Ca.* Kuenenia exhibits lower affinity constants for NH_4^+ and NO_2^-than *Ca.* Brocadia and *Ca.* Jettenia (Oshiki et al. 2016). Therefore, NxrT*, which clusters with NXR, may facilitate the growth of *Ca.* Kuenenia under substrate-limited conditions by directly accepting electrons from NxrC and transferring them to KsTH or NIR (Chicano et al. 2021).

Interestingly, Shaw et al. (Shaw et al. 2020), in their transcriptomic analysis of microbial electrolytic cell (MCE) experiments using external electrodes as the sole electron acceptor, observed that the activity of the kustc0458 gene, which catalyzes the conversion of NO_2^- to NO, as well as genes regulating the electron transport module, were significantly down-regulated in *Ca.* Brocadia BROELE01 compared to the system in which nitrite acted as the electron acceptor. This suggests that NO_2^- deficiency negatively affects the activity of key enzymes and electron transport within the cell. Upon reanalysis of their transcriptomic data, it was further revealed that the shuttle proteins KsTH and NaxLS, which provide electrons to the HZS, were also significantly down-regulated (Table S9), suggesting that NO_2^- deficiency severely disrupts the electron reflux system and impairs the activity of shuttle proteins.

3.4. *Sophisticated core anammox reaction endows Ca. Brocadiaceae with better adaptation to the wastewater system*

Compared with groundwater or marine ecosystem environments, the high concentration of NH_4^+-N, NO_x^--N and organic matter in wastewater (Hu et al. 2023; Yang et al. 2021). In addition, the competitive inhibition of N-related microorganisms, such as AOB/AOA, NOB, denitrifying bacteria, effectively impede the growth and metabolism of anammox bacteria, which is an important bottleneck of the practical application of the anammox process (Kuenen 2020; Yang et al. 2021). Therefore, the selection of suitable anammox bacteria as the initial bacterial agent is the key to start the anammox process. Combined with the ecological niche analysis, it was found that all the dominant anammox bacteria in wastewater belonged to the genus *Ca.* Brocadiaceae, including *Ca.* Kuenenia, *Ca.* Brocadia, *Ca.* Jettenia, and *Ca.* Loosdrechtia (Fig. 1a), which encode more mature anammox biochemical systems (Figs. 1a and 6). For instance, HZS was identified as the most important functional enzyme for the anammox core reaction, and interestingly, the dominant anammox flora in wastewater enhanced this reaction process by recruitment NaxLS and multicopy HZS (Figs. 1a and 6), which not only contributed to their rapid adaptation to the harsh wastewater environment, but also strengthened their ability to interact effectively with coexisting active microorganisms in the sludge (Hu et al. 2023; Yang et al. 2021),

To further characterize the transcription of the core anammox system of the genus *Ca.* Brocadiaceae in wastewater, we analyzed two WWTPs located in Guangzhou, China, and Zentraldeponie Emscherbruch, Germany. As shown in Fig. 7 and Table S7, all *Ca.* Brocadiaceae genus are obtained from this two WWTPs. Interestingly, we found that alterations in relative abundance affected the transcriptional activity of anammox bacterial core coding genes, particularly NXR and HZS (Fig. 7a). To further characterize the correlation, we subjected abundance and gene transcriptional activity to Pearson correlation analysis. The results showed that the abundance of *Ca.* Brocadiaceae was highly correlated with almost all core enzymes, with HZS, NXR, NaxL and NxrT being the most significant, followed by HDH, HOX, KsTH, and NaxS (Fig. 7b). This result suggests that nitrite oxidation and hydrazine synthesis are the two core biochemical reactions that determine the altered abundance of anammox bacteria. Meanwhile, NaxL, but not NaxS, was again confirmed to be the core shuttle protein mainly involved in HZS

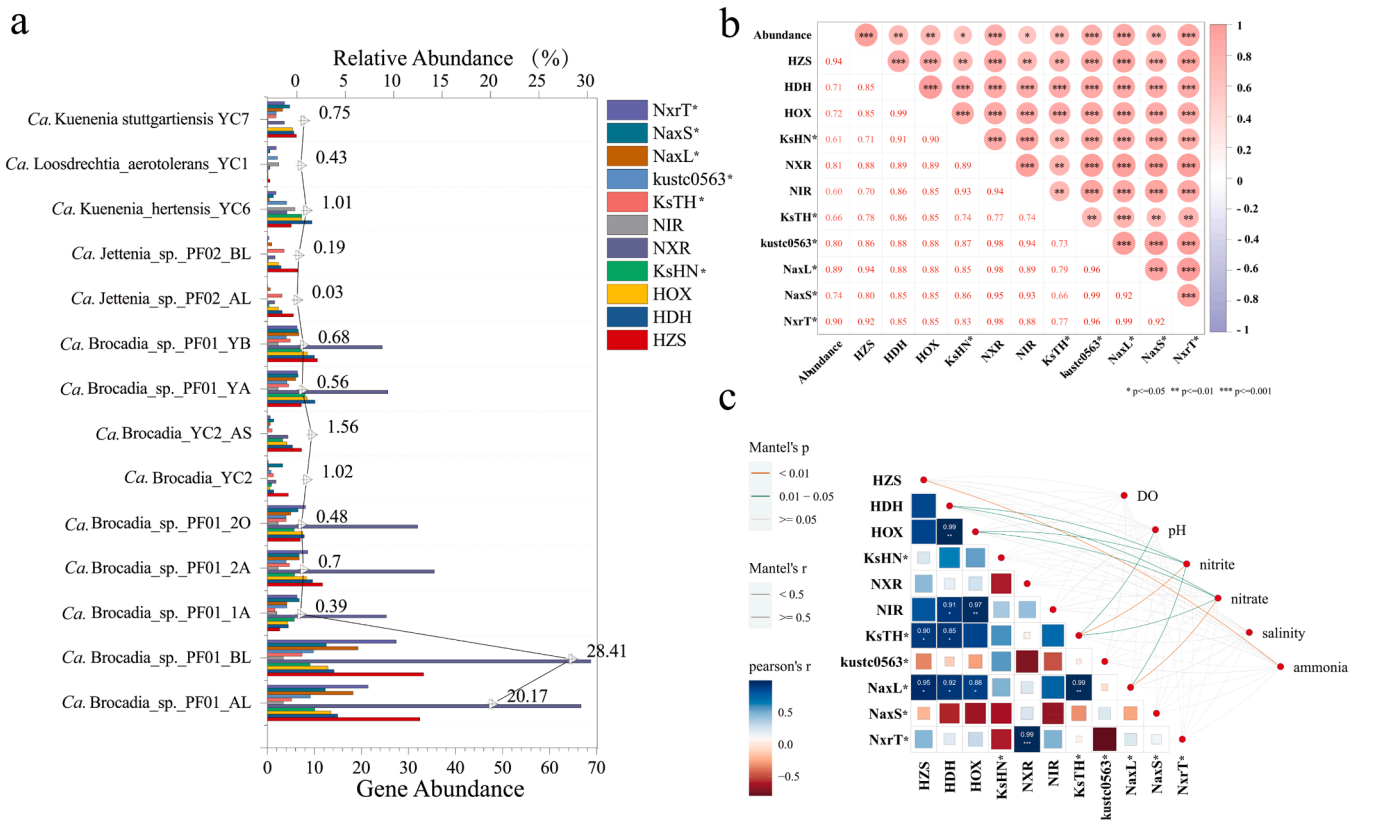

Fig. 7. Potential factors influencing the activity of key enzymes in wastewater. All Transcription and bacterial abundance of anammox bacterial core genes recovered from sludge and biofilm (a), correlation analysis of different enzyme activities with abundance in WWTPs (b), correlation analysis of different enzyme activities with environmental factors (c). AL: Aerobic tank biofilm A, BL: Aerobic tank biofilm B, 1A: Primary anoxic tank-sludge, 2A: Secondary anoxic tank-sludge, 2O: Secondary aerobic tank-sludge, YA: Primary aerobic tank A-sludge, YB: Primary aerobic tank B-sludge, AS: Activated sludge.

electron transfer, which is consistent with the results of our protein interaction simulation analysis (Fig. 3). Interestingly, the two enzymes responsible for the conversion of nitrite to NO, KsHN and NIR, had the lowest correlation with abundance (Fig. 7b). Previous studies have found that *Ca.* kuenenia can grow directly using NO as a substrate (Hu et al. 2019), so we hypothesize that the wastewater lineage *Ca.* Brocadiaceae can not only utilize environmental NO_2^- but also efficiently metabolize NO released by coexisting microorganisms. Subsequently, correlation analyses of environmental factors with core enzyme activities showed that pH, nitrate, nitrite, and ammonia concentrations all differentially affected the activity of one or several enzymes. Precisely, HZS activity showed a significant correlation with NH_4^+ concentration in the activate sludge (Fig. 7c), NO_2^- and NO_3^- concentrations were correlated with HDH, HOX, NaxL, and KsTH activities, and pH showed a correlation with KsTH (Fig. 7c). These results suggest that dynamically adjusting and monitoring these environmental factors can significantly enhance the enrichment of anammox bacteria and improve their metabolic efficiency. Unexpectedly, dissolved oxygen (DO) did not show any correlation with any relevant enzyme activity, which may be due to the regional limitation of the DO we monitored and further validation is needed regarding the correlation of DO with key enzymes due to the presence of fluctuating oxygen environments in the full-scale wastewater system as a result of sludge reflux or effluent-carried oxygen (Hu et al. 2023).

It is particularly noteworthy that most enzymes in the core redox reaction system, including NirS, HZS, HOX, KsHN, HDH, and electron shuttle proteins, are heme-type proteins (Akram et al. 2021; Akram et al. 2019a; Akram et al. 2019b; Kartal and Keltjens 2016; Klünemann and Blankenfeldt 2020). Therefore, effective enhancement of the biosynthesis capacity of heme-type proteins and the activity of these enzymes in anammox bacteria is an promising strategy to optimize the anammox reaction system. Previous studies have shown that iron (including Fe(II), Fe(III), Pyrite and iron nanoparticles) effectively promotes the enrichment of anaerobic bacteria and facilitates microbial intracellular electron transfer capacity as well as the efficiency of the anaerobic reaction by enhancing the biosynthesis of heme c and key enzymes (Table S8) (Ferousi et al. 2017; Wang et al. 2024; Wang et al. 2023b). Additionally, iron enters anammox cell through iron transporters on the cell membrane, enhancing the activity of genes regulating the iron transport system, such as the Feo system (*feoA* and *feoB*) and the ferrous uptake regulator (*Fur*) (Ferousi et al. 2017; Jiang et al. 2023), also facilitates the biosynthesis of the heme-like proteins in anammox bacterial cells.

4. Conclusions

In this study, the mechanism of the core anammox reactions and the evolutionary events of auxiliary electron transfer shuttle proteins in conjunction with geological events were investigated. The results indicate that different anammox bacterial lineages share similar core redox catalytic and electron transport mechanisms, while the electron transfer shuttle protein systems in anammox bacteria exhibited significant diversity. In particular, oxygen and nitrate/nitrite transformation are highly correlated with the modifications of the functional enzyme systems and the evolution of the electron transport shuttle protein system anammox bacteria over the geologic time. Furthermore, *in situ* transcriptome analysis based on two full-scale wastewater treatment systems revealed that HZS, NXR, NaxL, and NxrT activities were strongly correlated with anammox bacterial abundance, whereas nitrate, nitrite, and ammonia concentrations, as well as pH, influenced the function enzymes and shuttle protein activities. This study sheds new light on the biochemical processes of key redox enzymes in anammox bacteria and proposes the evolution changes of core biochemical enzymes in anammox bacteria under the dynamic changes of N over the Earth's geological age.

CRediT authorship contribution statement

Pengfei Hu: Writing – original draft, Visualization, Validation, Resources, Methodology, Investigation, Data curation, Conceptualization. **Mark van Loosdrecht:** Writing – review & editing, Conceptualization. **Ji-Dong Gu:** Writing – review & editing, Supervision, Funding acquisition, Data curation, Conceptualization. **Yuchun Yang:** Writing – review & editing, Methodology, Funding acquisition, Data curation.

Declaration of competing interest

The authors declare that they have no known competing financial interests or personal relationships that could have appeared to influence the work reported in this paper.

Acknowledgments

This study was funded by the National Natural Science Foundation of China (no 32470097, 32100086), National Key Research and Development Program of China (no 2021YFA0910300).

Supplementary materials

Supplementary material associated with this article can be found, in the online version, at doi:10.1016/j.watres.2025.123551.

Data availability

Data will be made available on request.

References

Aeschbach-Hertig, W., Gleeson, T., 2012. Regional strategies for the accelerating global problem of groundwater depletion. Nat. Geosci. 5 (12), 853–861.
Afanasieva, E., Chaudhuri, I., Martin, J., Hertle, E., Ursinus, A., Alva, V., Hartmann, M. D., Lupas, A.N., 2019. Structural diversity of oligomeric β-propellers with different numbers of identical blades. eLife 8, e49853.
Ağca, N., Karanlık, S., Ödemiş, B., 2014. Assessment of ammonium, nitrate, phosphate, and heavy metal pollution in groundwater from Amik Plain, southern Turkey. Environ. Monit. Assess. 186 (9), 5921–5934.
Akram, M., Bock, J., Dietl, A., Barends, T.R.M., 2021. Specificity of small c-type cytochromes in anaerobic ammonium oxidation. ACS Omega 6 (33), 21457–21464.
Akram, M., Dietl, A., Mersdorf, U., Prinz, S., Maalcke, W., Keltjens, J., Ferousi, C., de Almeida, N.M., Reimann, J., Kartal, B., Jetten, M.S.M., Parey, K., Barends, T.R., 2019a. A 192-heme electron transfer network in the hydrazine dehydrogenase complex. Sci. Adv. 5 (4), eaav4310.
Akram, M., Reimann, J., Dietl, A., Menzel, A., Versantvoort, W., Kartal, B., Jetten, M.S. M., Barends, T.R., 2019b. A nitric oxide-binding heterodimeric cytochrome c complex from the anammox bacterium Kuenenia stuttgartiensis binds to hydrazine synthase. J. Biolog. Chem. 294 (45), 16712–16728.
Almeida, N.M.d., Neumann, S., Mesman, R.J., Ferousi, C., Keltjens, J.T., Jetten, M.S.M., Kartal, B., Niftrik, L.v., 2015. Immunogold localization of key metabolic enzymes in the anammoxosome and on the tubule-like structures of *Kuenenia stuttgartiensis*. J. Bacteriol. 197 (14), 2432–2441.
Armstrong, C.T., Mason, P.E., Anderson, J.L.R., Dempsey, C.E., 2016. Arginine side chain interactions and the role of arginine as a gating charge carrier in voltage sensitive ion channels. Sci. Rep. 6 (1), 21759.
Arp, D.J., Chain, P.S.G., Klotz, M.G., 2007. The impact of genome analyses on our understanding of ammonia-oxidizing bacteria. Annu. Rev. Microbiol. 61 (1), 503–528.
Astashkin, A.V., Elmore, B.O., Chen, L., Fan, W., Guillemette, J.G., Feng, C., 2012. Pulsed ENDOR determination of the arginine location in the ferrous-NO form of neuronal NOS. J. Phys. Chem. A 116 (25), 6731–6739.
Bekker, A., Holland, H.D., 2012. Oxygen overshoot and recovery during the early Paleoproterozoic. Earth Planet Sci. Lett. 295–304, 317-318.
Benjamini, Y., Hochberg, Y., 2018. Controlling the false discovery rate: a practical and powerful approach to multiple testing. J. Roy. Statist. Soc.: Ser. B. (Methodolog.) 57 (1), 289–300.
Canfield, D.E., Zhang, S., Frank, A.B., Wang, X., Wang, H., Su, J., Ye, Y., Frei, R., 2018. Highly fractionated chromium isotopes in mesoproterozoic-aged shales and atmospheric oxygen. Nat. Commun. 9 (1), 2871.
Capella-Gutiérrez, S., Silla-Martínez, J.M., Gabaldón, T., 2009. trimAl: a tool for automated alignment trimming in large-scale phylogenetic analyses. Bioinformatics 25 (15), 1972–1973.

Cedervall, P., Hooper, A.B., Wilmot, C.M., 2013. Structural studies of hydroxylamine oxidoreductase reveal a unique heme cofactor and a previously unidentified interaction partner. Biochemistry 52 (36), 6211–6218.
Chen, C.K.M., Chan, N.-L., Wang, A.H.J., 2011. The many blades of the β-propeller proteins: conserved but versatile. Trend. Biochem. Sci. 36 (10), 553–561.
Chen, G., Cheng, Q., Lyons, T.W., Shen, J., Agterberg, F., Huang, N., Zhao, M., 2022. Reconstructing Earth's atmospheric oxygenation history using machine learning. Nat. Commun. 13 (1), 5862.
Chicano, T.M., Dietrich, L., de Almeida, N.M., Akram, M., Hartmann, E., Leidreiter, F., Leopoldus, D., Mueller, M., Sánchez, R., Nuijten, G.H.L., Reimann, J., Seifert, K.-A., Schlichting, I., van Niftrik, L., Jetten, M.S.M., Dietl, A., Kartal, B., Parey, K., Barends, T.R.M., 2021. Structural and functional characterization of the intracellular filament-forming nitrite oxidoreductase multiprotein complex. Nat. Microbiol. 6 (9), 1129–1139.
Colovos, C., Yeates, T.O., 1993. Verification of protein structures: patterns of nonbonded atomic interactions. Prot. Sci.: Public. Prot. Soc. 2 (9), 1511–1519.
de Almeida, N.M., Wessels, H.J.C.T., de Graaf, R.M., Ferousi, C., Jetten, M.S.M., Keltjens, J.T., Kartal, B., 2016. Membrane-bound electron transport systems of an anammox bacterium: a complexome analysis. Biochimica et Biophysica Acta (BBA) - Bioenerget. 1857 (10), 1694–1704.
Dietl, A., Ferousi, C., Maalcke, W.J., Menzel, A., de Vries, S., Keltjens, J.T., Jetten, M.S. M., Kartal, B., Barends, T.R., 2015. The inner workings of the hydrazine synthase multiprotein complex. Nature 527 (7578), 394–397.
Dietl, A., Maalcke, W.J., Ferousi, C., Jetten, M.S.M., Kartal, B., Barends, T.R., 2019. A 60-heme reductase complex from an anammox bacterium shows an extended electron transfer pathway. Acta Crystallogr. D Struct. Biol. 75 (Pt 3), 333–341.
Fernández, M.L., Estrin, D.A., Bari, S.E., 2008. Theoretical insight into the hydroxylamine oxidoreductase mechanism. J. Inorg. Biochem. 102 (7), 1523–1530.
Ferousi, C., Lindhoud, S., Baymann, F., Hester, E.R., Reimann, J., Kartal, B., 2019. Discovery of a functional, contracted heme-binding motif within a multiheme cytochrome. J. Biolog. Chem. 294 (45), 16953–16965.
Ferousi, C., Lindhoud, S., Baymann, F., Kartal, B., Jetten, M.S.M., Reimann, J., 2017. Iron assimilation and utilization in anaerobic ammonium oxidizing bacteria. Curr. Opin. Chem. Biol. 37, 129–136.
Ferousi, C., Schmitz, R.A., Maalcke, W.J., Lindhoud, S., Versantvoort, W., Jetten, M.S.M., Reimann, J., Kartal, B., 2021. Characterization of a nitrite-reducing octaheme hydroxylamine oxidoreductase that lacks the tyrosine cross-link. J. Biolog. Chem. 296.
Garcia, P.S., Jauffrit, F., Grangeasse, C., Brochier-Armanet, C., 2019. GeneSpy, a user-friendly and flexible genomic context visualizer. Bioinformatics 35 (2), 329–331.
Gori, F., Tringe, S.G., Kartal, B., Machiori, E., Jetten, M.S., 2011. The metagenomic basis of anammox metabolism in *Candidatus* 'Brocadia fulgida. Biochem. Soc. Trans. 39 (6), 1799–1804.
Hira, D., Toh, H., Migita, C.T., Okubo, H., Nishiyama, T., Hattori, M., Furukawa, K., Fujii, T., 2012. Anammox organism KSU-1 expresses a NirK-type copper-containing nitrite reductase instead of a NirS-type with cytochrome cd 1. FEBS Lett. 586 (11), 1658–1663.
Horton, F., 2015. Did phosphorus derived from the weathering of large igneous provinces fertilize the neoproterozoic ocean? Geochemistry,. Geophysics,. Geosystems. 16 (6), 1723–1738.
Hu, P., Qian, Y., Liu, J., Gao, L., Li, Y., Xu, Y., Wu, J., Hong, Y., Ford, T., Radian, A., Yang, Y., Gu, J.-D., 2023. Delineation of the complex microbial nitrogen-transformation network in an anammox-driven full-scale wastewater treatment plant. Water Res. 235, 119799.
Hu, Z., Wessels, H.J.C.T., van Alen, T., Jetten, M.S.M., Kartal, B., 2019. Nitric oxide-dependent anaerobic ammonium oxidation. Nat. Commun. 10 (1), 1244.
Hyatt, D., Chen, G.-L., LoCascio, P.F., Land, M.L., Larimer, F.W., Hauser, L.J., 2010. Prodigal: prokaryotic gene recognition and translation initiation site identification. BMC Bioinformat. 11 (1), 119.
Igarashi, N., Moriyama, H., Fujiwara, T., Fukumori, Y., Tanaka, N., 1997. The 2.8 Å structure of hydroxylamine oxidoreductase from a nitrifying chemoautotrophic bacterium, Nitrosomonas europaea. Nat. Struct. Mol. Biol. 4 (4), 276–284.
Jiang, Y., Chen, Y., Wang, Y., Chen, X., Zhou, X., Qing, K., Cao, W., Zhang, Y., 2023. Novel insight into the inhibitory effects and mechanisms of Fe(II)-mediated multi-metabolism in anaerobic ammonium oxidation (anammox). Water Res. 242, 120291.
Kalyaanamoorthy, S., Minh, B.Q., Wong, T.K.F., von Haeseler, A., Jermiin, L.S., 2017. ModelFinder: fast model selection for accurate phylogenetic estimates. Nat. Method. 14 (6), 587–589.
Kartal, B., Keltjens, J.T., 2016. Anammox biochemistry: a tale of heme c proteins. Trend. Biochem. Sci. 41 (12), 998–1011.
Kartal, B., Maalcke, W., Almeida, N., Cirpus, I., Gloerich, J., Geerts, W., Op den Camp, H., Harhangi, H., Janssen-Megens, E., Francoijs, K.-J., Stunnenberg, H., Keltjens, J., Jetten, M., Strous, M., 2011a. Molecular mechanism of anaerobic ammonium oxidation. Nature 479, 127–130.
Katoh, K., Misawa, K., Kuma, K.i., Miyata, T., 2002. MAFFT: a novel method for rapid multiple sequence alignment based on fast fourier transform. Nucl. Acid. Res. 30 (14), 3059–3066.
Kim, H.J., Khalimonchuk, O., Smith, P.M., Winge, D.R., 2012. Structure, function, and assembly of heme centers in mitochondrial respiratory complexes. Biochimica et Biophysica Acta (BBA) - Molecul. Cell Res. 1823 (9), 1604–1616.
Klünemann, T., Blankenfeldt, W., 2020. Structure of heme d(1)-free cd(1) nitrite reductase NirS. Acta Crystallogr. F Struct. Biol. Commun. 76, 250–256. Pt 6.
Knoll, A.H., Nowak, M.A., 2017. The timetable of evolution. Sci. Adv. 3 (5), e1603076.
Kopylova, E., Noé, L., Touzet, H., 2012. SortMeRNA: fast and accurate filtering of ribosomal RNAs in metatranscriptomic data. Bioinformatics 28 (24), 3211–3217.
Kuenen, J.G., 2008. Anammox bacteria: from discovery to application. Nat. Rev. Microbiol. 6 (4), 320–326.
Kuenen, J.G., 2020. Anammox and beyond. Environ. Microbiol. 22 (2), 525–536.
Kuypers, M.M.M., Marchant, H.K., Kartal, B., 2018. The microbial nitrogen-cycling network. Nat. Rev. Microbiol. 16 (5), 263–276.
Letunic, I., Bork, P., 2021. Interactive Tree of Life (iTOL) v5: an online tool for phylogenetic tree display and annotation. Nucl. Acid. Res. 49 (W1), W293–W296.
Li, D., Liu, C.-M., Luo, R., Sadakane, K., Lam, T.-W., 2015. MEGAHIT: an ultra-fast single-node solution for large and complex metagenomics assembly via succinct de Bruijn graph. Bioinformatics 31 (10), 1674–1676.
Li, T., Bonkovsky, H.L., Guo, J., 2011. Structural analysis of heme proteins: implications for design and prediction. BMC Struct. Biol. 11 (1), 13.
Liao, T., Wang, S., Stüeken, E.E., Luo, H., 2022. Phylogenomic evidence for the origin of obligate Anaerobic anammox bacteria around the great oxidation event. Mol. Biol. Evol. 39 (8).
Liu, T., Lu, Y., Zheng, M., Hu, S., Yuan, Z., Guo, J., 2021. Efficient nitrogen removal from mainstream wastewater through coupling Partial nitritation, Anammox and Methane-dependent nitrite/nitrate reduction (PNAM). Water Res. 206, 117723.
Maalcke, W.J., Dietl, A., Marritt, S.J., Butt, J.N., Jetten, M.S., Keltjens, J.T., Barends, T. R., Kartal, B., 2014. Structural basis of biological NO generation by octaheme oxidoreductases. J. Biolog. Chem. 289 (3), 1228–1242.
Mahram, A., Herbordt, M.C., 2015. NCBI BLASTP on high-performance reconfigurable computing systems. ACM Trans. Reconfigur. Technol. Syst. 7 (4), 33.
Minh, B.Q., Schmidt, H.A., Chernomor, O., Schrempf, D., Woodhams, M.D., von Haeseler, A., Lanfear, R., 2020. IQ-TREE 2: new models and efficient methods for phylogenetic inference in the genomic era. Mol. Biol. Evol. 37 (5), 1530–1534.
Mirdita, M., Schütze, K., Moriwaki, Y., Heo, L., Ovchinnikov, S., Steinegger, M., 2022. ColabFold: making protein folding accessible to all. Nat. Method. 19 (6), 679–682.
Nurizzo, D., Silvestrini, M.-C., Mathieu, M., Cutruzzolà, F., Bourgeois, D., Fülöp, V., Hajdu, J., Brunori, M., Tegoni, M., Cambillau, C., 1997. N-terminal arm exchange is observed in the 2.15A crystal structure of oxidized nitrite reductase from *Pseudomonas aeruginosa*. Structure 5 (9), 1157–1171.
Okubo, T., Toyoda, A., Fukuhara, K., Uchiyama, I., Harigaya, Y., Kuroiwa, M., Suzuki, T., Murakami, Y., Suwa, Y., Takami, H., 2020. The physiological potential of anammox bacteria as revealed by their core genome structure. DNA Res. 28 (1).
Opperman, D.J., Murgida, D.H., Dalosto, S.D., Brondino, C.D., Ferroni, F.M., 2019. A three-domain copper-nitrite reductase with a unique sensing loop. IUCrJ. 6 (Pt 2), 248–258.
Oshiki, M., Satoh, H., Okabe, S., 2016. Ecology and physiology of anaerobic ammonium oxidizing bacteria. Environ. Microbiol. 18 (9), 2784–2796.
Palomo, A., Azevedo, D., Touceda-Suárez, M., Domingo-Félez, C., Mutlu, A.G., Dechesne, A., Wang, Y., Zhang, T., Smets, B.F., 2022. Efficient management of the nitritation-anammox microbiome through intermittent aeration: absence of the NOB guild and expansion and diversity of the NO_x reducing guild suggests a highly reticulated nitrogen cycle. Environ. Microb. 17 (1), 39.
Parks, D., Imelfort, M., Skennerton, C., Philip, H., Tyson, G., 2015. CheckM: assessing the quality of microbial genomes recovered from isolates, single cells, and metagenomes. Genom. Res. 25.
Pierce, B.G., Wiehe, K., Hwang, H., Kim, B.H., Vreven, T., Weng, Z., 2014. ZDOCK server: interactive docking prediction of protein-protein complexes and symmetric multimers. Bioinformatics 30 (12), 1771–1773.
Pontius, J., Richelle, J., Wodak, S.J., 1996. Deviations from standard atomic volumes as a quality measure for protein crystal structures. J. Mol. Biol. 264 (1), 121–136.
Poulton, S.W., Fralick, P.W., Canfield, D.E., 2010. Spatial variability in oceanic redox structure 1.8 billion years ago. Nat. Geosci. 3 (7), 486–490.
Rich, J.J., Arevalo, P., Chang, B.X., Devol, A.H., Ward, B.B., 2020. Anaerobic ammonium oxidation (anammox) and denitrification in Peru margin sediments. J. Marin. Syst. 207, 103122.
Rockström, J., Steffen, W., Noone, K., Persson, Å., Chapin, F.S., Lambin, E.F., Lenton, T. M., Scheffer, M., Folke, C., Schellnhuber, H.J., Nykvist, B., de Wit, C.A., Hughes, T., van der Leeuw, S., Rodhe, H., Sörlin, S., Snyder, P.K., Costanza, R., Svedin, U., Falkenmark, M., Karlberg, L., Corell, R.W., Fabry, V.J., Hansen, J., Walker, B., Liverman, D., Richardson, K., Crutzen, P., Foley, J.A., 2009. A safe operating space for humanity. Nature 461 (7263), 472–475.
Sarkar, A., Bhakta, S., Chattopadhyay, S., Dey, A., 2023. Role of distal arginine residue in the mechanism of heme nitrite reductases. Chem. Sci. 14 (29), 7875–7886.
Schmid, M., Walsh, K., Webb, R., Rijpstra, W.I., van de Pas-Schoonen, K., Verbruggen, M. J., Hill, T., Moffett, B., Fuerst, J., Schouten, S., Sinninghe Damsté, J.S., Harris, J., Shaw, P., Jetten, M., Strous, M., 2003. *Candidatus* "Scalindua brodae", sp. nov., *Candidatus* "Scalindua wagneri", sp. nov., two new species of Anaerobic ammonium oxidizing bacteria. Syst. Appl. Microbiol. 26 (4), 529–538.
Shaw, D.R., Ali, M., Katuri, K.P., Gralnick, J.A., Reimann, J., Mesman, R., van Niftrik, L., Jetten, M.S.M., Saikaly, P.E., 2020. Extracellular electron transfer-dependent anaerobic oxidation of ammonium by anammox bacteria. Nat. Commun. 11 (1), 2058.
Spalding, R.F., Hirsh, A.J., Exner, M.E., Little, N.A., Kloppenborg, K.L., 2019. Applicability of the dual isotopes δ15N and δ18O to identify nitrate in groundwater beneath irrigated cropland. J. Contam. Hydrol. 220, 128–135.
Stüeken, E.E., Kipp, M.A., Koehler, M.C., Buick, R., 2016. The evolution of Earth's biogeochemical nitrogen cycle. Earth-Sci. Rev. 160, 220–239.
Stüeken, E.E., Pellerin, A., Thomazo, C., Johnson, B.W., Duncanson, S., Schoepfer, S.D., 2024. Marine biogeochemical nitrogen cycling through Earth's history. Nat. Rev. Earth Environ. 5 (10), 732–747.
Subba Rao, A., Jha, P., Meena, B.P., Biswas, A.K., Lakaria, B.L., Patra, A.K., 2017. In: Abrol, Y.P., Adhya, T.K., Aneja, V.P., Raghuram, N., Pathak, H., Kulshrestha, U., Sharma, C., Singh, B. (Eds.), The Indian Nitrogen Assessment. Elsevier, pp. 59–76.

Tamura, K., Stecher, G., Kumar, S., 2021. MEGA11: molecular Evolutionary Genetics Analysis Version 11. Mol. Biol. Evol. 38 (7), 3022–3027.
Tao, J., Zhang, J., Liu, Y., Stüeken, E.E., Dong, Z., Shi, M., Li, P., Zhang, Q., Poulton, S. W., 2022. A stable and moderate nitrate pool in largely anoxic mesoproterozoic oceans and implications for eukaryote evolution. Precambr. Res. 381, 106868.
Ukita, S., Fujii, T., Hira, D., Nishiyama, T., Kawase, T., Migita, C.T., Furukawa, K., 2010. A heterodimeric cytochrome c complex with a very low redox potential from an anaerobic ammonium-oxidizing enrichment culture. FEMS Microbiol. Lett. 313 (1), 61–67.
Uritskiy, G.V., DiRuggiero, J., Taylor, J., 2018. MetaWRAP-a flexible pipeline for genome-resolved metagenomic data analysis. Microbiome 6 (1), 158.
van de Vossenberg, J., Woebken, D., Maalcke, W.J., Wessels, H.J.C.T., Dutilh, B.E., Kartal, B., Janssen-Megens, E.M., Roeselers, G., Yan, J., Speth, D., Gloerich, J., Geerts, W., van der Biezen, E., Pluk, W., Francoijs, K.-J., Russ, L., Lam, P., Malfatti, S. A., Tringe, S.G., Haaijer, S.C.M., Op den Camp, H.J.M., Stunnenberg, H.G., Amann, R., Kuypers, M.M.M., Jetten, M.S.M., 2013. The metagenome of the marine anammox bacterium '*Candidatus* Scalindua profunda' illustrates the versatility of this globally important nitrogen cycle bacterium. Environ. Microbiol. 15 (5), 1275–1289.
Varsadiya, M., Urich, T., Hugelius, G., Bárta, J., 2021. Fungi in permafrost-affected soils of the canadian Arctic: horizon- and site-specific keystone taxa revealed by Co-occurrence network. Microorganisms 9 (9).
Wang, X., Zhang, S., Ye, Y., Ma, S., Su, J., Wang, H., Canfield, D.E., 2023. Nitrogen cycling during the Mesoproterozoic as informed by the 1400 million year old Xiamaling Formation. Earth-Sci. Rev. 243, 104499.
Wang, S., Zhang, K., Miao, Y., Wang, Z., 2024. The enhancement of anammox by graphene-based and iron-based nanomaterials in performance and mechanisms. npj Clean. Water 7 (1), 100.
Wu, J., Yang, Y., Gu, J.-D., Hong, Y., 2023. Novel anammox bacteria discovered in the untapped subsurface aquifers. bioRxiv, 2023.2004.2027.538623.
Yang, Y., Azari, M., Herbold, C.W., Li, M., Chen, H., Ding, X., Denecke, M., Gu, J.-D., 2021. Activities and metabolic versatility of distinct anammox bacteria in a full-scale wastewater treatment system. Water Res. 206, 117763.
Yang, Y., Lu, Z., Azari, M., Kartal, B., Du, H., Cai, M., Herbold, C.W., Ding, X., Denecke, M., Li, X., Li, M., Gu, J.D., 2022. Discovery of a new genus of anaerobic ammonium oxidizing bacteria with a mechanism for oxygen tolerance. Water Res. 226, 119165.
Yang, Y., Pan, J., Zhou, Z., Wu, J., Liu, Y., Lin, J.-G., Hong, Y., Li, X., Li, M., Gu, J.-D., 2020. Complex microbial nitrogen-cycling networks in three distinct anammox-inoculated wastewater treatment systems. Water Res. 168, 115142.
Yuan, S., Chan, H., Filipek, S., Vogel, H., 2016. PyMOL and Inkscape bridge the data and the data visualization. Structure 24.
Zhang, M., Wang, S., Ji, B., Liu, Y., 2019. Towards mainstream deammonification of municipal wastewater: partial nitrification-anammox *versus* partial denitrification-anammox. Sci. Total Environ. 692, 393–401.
Zhao, R., Biddle, J.F., Jørgensen, S.L., 2022. Introducing *Candidatus* Bathyanammoxibiaceae, a family of bacteria with the anammox potential present in both marine and terrestrial environments. ISME Commun. 2 (1), 42.
Zhuang, J.-L., Sun, X., Zhao, W.-Q., Zhang, X., Zhou, J.-J., Ni, B.-J., Liu, Y.-D., Shapleigh, J.P., Li, W., 2022. The anammox coupled partial-denitrification process in an integrated granular sludge and fixed-biofilm reactor developed for mainstream wastewater treatment: performance and community structure. Water Res. 210, 117964.